Published in final edited form as:
J Bone Miner Res. 2013 June ; 28(6): 1489–1500. doi:10.1002/jbmr.1884.

Role of ATF7-TAF12 interactions in the VDR hyper-sensitivity of osteoclast precursors in Paget's disease

Jumpei Teramachi[1], **Yuko Hiruma**[2], **Seiichi Ishizuka**[2], **Hisako Ishizuka**[2], **Jacques P. Brown**[3], **Laëtitia Michou**[3], **Huiling Cao**[2], **Deborah L Galson**[2], **Mark A Subler**[4], **Hua Zhou**[5], **David W Dempster**[5], **Jolene J Windle**[4], **G. David Roodman**[1], and **Noriyoshi Kurihara**[1]

[1]Department of Medicine/Hem-Onc, Indiana University, Indianapolis, IN

[2]Department of Medicine/Hem-Onc, University of Pittsburgh and the Center for Bone Biology at UPMC, Pittsburgh, PA

[3]Laval University, CHUQ-CHUL Research Center, Quebec, QC, Canada

[4]Department of Human and Molecular Genetics, Virginia Commonwealth University, Richmond, VA

[5]Department of Pathology, College of Physician and Surgeons, Columbia University, New York, NY

Abstract

Osteoclast (OCL) precursors from many Paget's disease (PD) patients express measles virus nucleocapsid protein (MVNP) and are hypersensitive to 1,25-$(OH)_2D_3$. The increased 1,25-$(OH)_2D_3$ sensitivity is mediated by TAF12, a co-activator of VDR, which is present at much higher levels in MVNP-expressing OCL precursors than normals. These results suggest that TAF12 plays an important role in the abnormal OCL activity in PD. However, the molecular mechanisms underlying both 1,25-$(OH)_2D_3$'s effects on OCL formation and the contribution of TAF12 to these effects in both normals and PD patients are unclear. Inhibition of TAF12 with a specific *TAF12* antisense construct decreased OCL formation and OCL precursors sensitivity to 1,25-$(OH)_2D_3$ in PD patient bone marrow samples. Further, OCL-precursors from transgenic mice in which *TAF12* expression was targeted to the OCL lineage (TRAP-*TAF12* mice), formed OCL at very low levels of 1,25-$(OH)_2D_3$, although the OCL failed to exhibit other hallmarks of PD OCL, including RANKL hyper-sensitivity and hyper-multinucleation. ChIP analysis of OCL precursors using an anti-TAF12 antibody demonstrated that TAF12 binds the *24-hydroxylase* (*CYP24A1*) promoter, which contains two functional vitamin D response elements (VDRE), in the presence of 1,25-$(OH)_2D_3$. Since TAF12 directly interacts with the ATF7 transcription factor and potentiates ATF7-induced transcriptional activation of ATF7-driven genes in other cell types, we determined if TAF12 is a functional partner of ATF7 in OCL precursors. Immunoprecipitation of lysates from either WT or *MVNP*-expressing OCL with an anti-TAF12 antibody followed by blotting with an anti-ATF7 antibody, or vice versa, showed that TAF12 and ATF7 physically interact in OCL. Knockdown of *ATF7* in *MVNP*-expressing cells decreased CYP24A1 induction by 1,25-$(OH)_2D_3$ as well as TAF12 binding to the *CYP24A1* promoter. These results show that ATF7 interacts with TAF12 and contributes to the hyper-sensitivity of OCL precursors to 1,25-$(OH)_2D_3$ in PD.

DISCLOSURES

GDR is a consult to Amgen and develops continuing medical education material for Clinical Care Options. All other authors state that they have no conflicts of interest.

Keywords

TAF12; Vitamin D; Paget's Disease; Osteoclasts; ATF7

INTRODUCTION

Paget's disease (PD) is a very common bone disease that affects 1–2 million Americans. It is one of the most exaggerated forms of coupled bone remodeling in which excessive bone resorption is followed by exuberant bone formation and provides important insights into the normal bone remodeling process (1, 2). Studies of PD have revealed that 1,25-$(OH)_2D_3$ can act directly on OCL precursors to induce OCL formation independent of RANKL, and that OCL precursors from PD patients form OCL at physiologic (10^{-11}M) rather than the pharmacologic (10^{-8}M) concentrations of 1,25-$(OH)_2D_3$ required for normal OCL precursors (3). This enhanced sensitivity on OCL precursors to 1,25-$(OH)_2D_3$ in PD results from increased expression of TAF12 (formerly TAF_{II}-17), a member of the TFIID transcription factor complex (4–6). TAF12 acts as a co-activator of the vitamin D receptor (VDR), and increased levels of TAF12 enhance the VDR responsivity of OCL precursors from PD patients (7). However, the molecular mechanisms regulating TAF12's effects on genes activated by 1,25-$(OH)_2D_3$/VDR in OCL are undefined.

We and others have previously shown that both environmental factors, in particular measles virus, and genetic factors, such as mutant p62/sequestosome 1 (e.g., $p62^{P392L}$), both contribute to the pathogenesis of PD (8–10). However, genetic factors alone do not appear to be sufficient to induce PD. We reported that transfection of the $p62^{P392L}$ gene into normal OCL precursors does not result in formation of pagetic-like OCLs *in vitro*. Importantly, OCL from transgenic mice overexpressing the *$p62^{P392L}$* mutation or *$p62^{P394L}$* knock in mice do not express elevated TAF12, are not hypersensitive to 1,25$(OH)_2D_3$, and in our experience do not develop pagetic bone lesions (11).

In contrast, transfection of normal OCL precursors with the measles virus nucleocapsid protein (MVNP) gene results in development of OCL which exhibit most of the characteristics of PD OCL, including increased TAF12 expression and VDR hyper-sensitivity in OCL precursors as well as other cell types (8). Further, targeting MVNP to the OCL lineage in transgenic mice (TRAP-*MVNP* mice) induces formation of bone lesions and OCL characteristic of PD (10). Thus, TRAP-*MVNP* mice provide us an in vivo model to further explore the molecular mechanisms responsible for vitamin D_3's effects on OCL formation and activity in PD as well as in normal bone remodeling. We recently showed that blocking MVNP expression in MVNP-positive OCL from PD patients using an antisense construct resulted in loss of the pagetic phenotype and reduced TAF12 expression, regardless of whether the OCL also harbored a p62 mutation (8). However, the role that TAF12 and 1,25-$(OH)_2D_3$ hyper-sensitivity play in the development of the "pagetic phenotype" in OCL and PD is still unclear.

Previous studies showed that TAF12 levels were increased in colorectal cancer cells harboring a RAS mutation, and that TAF12 levels were reduced when the cells were treated with a MEK inhibitor (13). Further, TAF12 over-expression was found to potentiate ATF7-induced transcriptional activation through direct interaction in colorectal cancer cells, and this effect was inhibited by TAF4, which blocks the interaction between TAF12 and ATF7 (12).

Therefore, we examined the role of TAF12 and ATF7 in VDR-mediated OCL formation, using both human CFU-GM (a highly purified population of early-osteoclast precursors)

transduced with a *TAF12* retrovirus, and OCL precursors from transgenic mice with *TAF12* expression targeted to the OCL. We found that ATF7 physically interacts with TAF12 and increases TAF12 levels in OCL precursors, contributes to the 1,25-$(OH)_2D_3$ hyper-sensitivity of OCL precursors induced by TAF12, and that OCL from TRAP-*TAF12* mice were hyper-sensitive to 1,25-$(OH)_2D_3$ and produced increased levels of IL-6 compared to WT mice. However, increased expression of TAF12 by itself was not sufficient to induce hyper-multinucleated OCL or pagetic bone lesions, demonstrating that other factors in addition to increased TAF12 expression are required to induce pagetic OCL and bone lesions.

EXPERIMENTAL PROCEDURES

OCL formation by PD and normal OCL precursors transduced with AS-*TAF12* or scrambled antisense to *TAF12*

Human marrow mononuclear cells isolated from involved sites of three $MVNP^+$ Paget's patients and two normals were cultured for 96 hr with cytokines and the retroviral supernatants as previously described (8). These studies were approved by the Institutional Review Board at the University of Pittsburgh. The cells were resuspended at 2.5×10^6 cells / ml and were cultured in α-Minimal Essential Medium (α-MEM, Gibco BRL Invitrogen, Carlsbad, CA, USA) containing 10% fetal bovine serum (FBS, Invitrogen) plus 10 ng/ml each of IL-3, IL-6 and stem cell growth factor for 2 days to induce proliferation of hematopoietic precursors. The marrow cells were then transduced with retroviral vectors that contained a neomycin resistance gene and the human AS-*TAF12* (*pCMV/*AS-*TAF12*) *or scrambled antisense TAF12* (pCMV/scrambled AS-*TAF12*). The transduced cells were cultured in methylcellulose with human GM-CSF (200 pg/ml) in the presence of 250 pg/ml G418 to select for CFU-GM colonies that expressed AS-*TAF12* or scrambled AS-*TAF12*. CFU-GM colony derived cells that expressed AS-*TAF12* or scrambled AS-*TAF12* (2×10^5 cells/well: 96-well plate) were cultured in α-MEM+20% horse serum for 21 days in the presence of varying concentrations of 1,25-$(OH)_2D_3$. Cells were then stained for 23C6 (CD51) using a Vectastain® kit (Vector Laboratory), and $23C6^+$ multinucleated cells (≥ 3 nuclear/ cells) were counted as OCL (8).

OCL formation by normal human OCL precursors transduced with the *TAF12* gene or empty vector

Non-adherent mononuclear human marrow cells were collected by bone marrow aspiration from normal volunteers as previously described (8). These studies were approved by the Institutional Review Board at the University of Pittsburgh. The cells were resuspended at 2.5×10^6 cells /ml and were cultured in α-MEM containing 10% FBS plus 10 ng/ml each of IL-3, IL-6 and stem cell growth factor for 2 days to induce proliferation of hematopoietic precursors. The marrow cells were then transduced with retroviral vectors that contained a neomycin resistance gene and the human *TAF12* cDNA (*pCMV/TAF12*), *MVNP* (*pCMV/MVNP*) *or empty vector* (*EV*) (9, 14). The transduced cells were cultured for OCL formation as descried above.

Development of TRAP-TAF12 transgenic mice

All studies were approved by the IACUCs at both the University of Pittsburgh School of Medicine and Virginia Commonwealth University. To generate the TRAP-*TAF12* transgene construct, a 0.5-kb human *TAF12* cDNA (originally derived from a Paget's patient) was inserted into the unique EcoRI site of the pKCR3-mTRAP vector (15, 16). pKCR3-m*TRAP* contains 1.9 kb of the mouse TRAP gene promoter and 5′-UTR, in addition to rabbit β-globin intron 2 and its flanking exons (for efficient transgene expression). A 3.6-kb injection fragment was then excised from the TRAP-*TAF12* construct with *XhoI*, and transgenic mice

were generated by standard methods in a CB6F1 (C57Bl/6 × Balb/c) genetic background (17). Potential founders were screened for the presence of the TRAP-*TAF12* transgene by PCR analysis of genomic tail DNA using a mouse *TRAP* sense primer (5'-CTGGACAATCCTCGGAGAAAATGC-3') and a rabbit β-globin anti-sense primer (5'-GCGAAAAAGAAAGAACAATCAAG-3'). Amplification of DNA from mice carrying the TRAP-*TAF12* transgene generated a 591-bp PCR product. Founders were bred to establish multiple independent lines of mice. To verify the integrity of the TRAP-*TAF12* transgene, Southern blot analysis of DNA from founders and their progeny was performed using the *XhoI* injection fragment as probe.

Osteoclast formation from transgenic mouse bone marrow

Bone marrow cells were flushed from long bones of WT, TRAP-*TAF1*2 or TRAP-*MVNP* (10) mice of various ages and plated on 100-mm tissue culture plates in α-MEM containing 10% FBS. Cells were incubated at 37°C in 5% CO_2 overnight. Non-adherent cells were harvested and enriched for $CD11b^+$ mononuclear cells using the Miltenyi Biotec MACS (Magnetic Cell Sorting) system (7). $CD11b^+$ cells then were cultured in α-MEM containing 10% FBS plus 10ng/mL of macrophage colony-stimulating factor (M-CSF; R&D) for 3 days to generate a population of enriched early OCL precursors. These were then cultured in α-MEM containing 10% FBS in the presence of 1,25-$(OH)_2D_3$ (Teijin Pharma, Tokyo) for 3 to 4 days to generate OCLs, and cells were then stained for TRAP using a leukocyte acid phosphatase kit (Sigma), TRAP-positive cells (≥ 3 nuclei/ cell) were scored microscopically.

Bone resorption assays of cultured OCLs

$CD11b^+$ cells were cultured on mammoth dentin slices (Wako, Osaka, Japan) in α-MEM containing 10% FCS and 1,25-$(OH)_2D_3$ (10^{-8} M). After 14 days of culture, the cells were removed, the dentin slices were stained with acid hematoxylin, and the areas of dentin resorption were determined using image-analysis techniques (NIH Image System) (8).

ChIP assays

ChIP assays were performed as described previously using osteoclast precursors from TRAP-*MVNP* or WT mice (18, 19). The equivalent of 10 μg DNA was used as starting material (input) in each ChIP reaction. The DNA was fragmented by sonification and then immuno-precipitated with 2 μg of anti-TAF12 antibody (Protein Tech Group. Inc). Portions of the ChIP DNA fractions (5%) or starting DNA (0.02%–0.05%) were used for PCR analysis. The reaction was performed with AmpliTaq Gold DNA Polymerase (Applied Biosystems) for 35 cycles of 60 seconds at 95°C, 90 seconds at 58°C, and 120 seconds at 68°C. The gene-specific primers for mouse *CYP24A1* mRNA were 5'-ATT ACC TGA GAA TCA GAG GCC ACG-3' (sense) and 5'-GCC AAA TGC AGT TTA AGC TCT GCT-3' (antisense). The PCR products were separated on 2% agarose gels and visualized with ultraviolet light. All ChIP assays were repeated at least 3 times.

Quantitative RT-PCR analysis

$CD11b^+$ cells from human bone marrow were cultured with 1,25-$(OH)_2D_3$ or vehicle for 2 days and subjected to reverse transcription PCR (RT-PCR) analysis for expression of *CYP24A1* mRNA. Total RNA was extracted using RNAzol B solution (Tel-Test Inc., Griendswood, TX, USA) and cDNAs were synthesized using an RNA PCR Kit (Applied Biosystems, Foster City, CA, USA). The gene-specific primers for mouse *CYP24A1* mRNA were 5'-ATT ACC TGA GAA TCA GAG GCC ACG-3' (sense) and 5'-GCC AAA TGC AGT TTA AGC TCT GCT-3' (antisense). The gene-specific primers for mouse β-actin were 5'-GGC CGT ACC ACT GGC ATC GTG ATG-3' (sense) and 5'-CTT GGC CGT CAG GCA GCT CGT AGC-3' (antisense).

Immunoblotting of OCL precursor lysates from WT, TRAP-*MVNP* or TRAP-*TAF12* mice

OCL precursors from WT, TRAP-*MVNP* or TRAP-*TAF12* mice were washed twice with ice-cold PBS (phosphate buffered saline), and were then lysed in buffer containing 20mM Tris, pH 7.5, 150mM NaCl, 1mM ethylenediaminetetraacetic acid (EDTA), 1mM EGTA [ethylene glycol-bis-(2-aminoethyl)-N,N,N', N'-tetraacetic acid], 1% Triton X-100, 2.5mM sodium pyrophosphate, 1mM β-glycerophosphate, 1mM Na_3VO_4, 1mM NaF, and ×1 protease inhibitor mixture. Cell lysates (50 μg) were boiled in the presence of sodium dodecyl sulfate (SDS) sample buffer [0.5 M Tris–HCl, pH 6.8, 10% (w/v) SDS, 10% glycerol, 0.05% (w/v) bromphenol blue] for 5 min and subjected to electrophoresis on 4–20% SDS–PAGE (Bio-Rad). Proteins were transferred to nitrocellulose membranes using a semi-dry blotter (Bio-Rad) and incubated in blocking solution (5% non-fat dry milk in TBS containing 0.1% Tween-20) for 1hour to reduce non-specific binding. Membranes were then exposed to primary antibodies overnight at 4°C, washed three times, and incubated with secondary goat anti-mouse or rabbit IgG HRP-conjugated antibody for 1hour. Membranes were washed extensively, and an enhanced chemiluminescence detection assay was performed following the manufacturer's directions (Bio-Rad). All blots were densitometrically quantitated and the results expressed relative to control and normalized to β-actin or TFIIB (Santa Cruz).

IL-6 ELISA assay

Conditioned media from mouse OCL cultures was harvested 7 days after the addition of 1,25-$(OH)_2D_3$. The concentration of IL-6 present was determined using an ELISA kit for mouse IL-6 (R&D), according to the manufacturer's instructions and were normalized to cell number.

ATF7 shRNA transduction

Non-adherent bone marrow cells from TRAP-MVNP and WT mice were transduced with *ATF7* shRNA (NM_146065) (Sigma-Aldrich) or control shRNA (Sigma-Aldrich) which were designed by MISSION®. The shRNA Lentiviral transduction particles (Sigma-Aldrich) were used for transduction. The transduction was performed by the MagnetoFection™-ViroMag R/L methods (OZ Biosciences), according to the manufacturer's instructions (20, 21). To increase the transduction efficiency, the cells were plated the day before transduction in 96 well culture plate in the presence of 10 ng/ml of M-CSF and 2 μl of ViroMag R/L beads in 50 pl of αMEM 10%FCS containing 10 ng/ml of M-CSF, 500 MOI of Lentiviral transduction particles were added, and the cells incubated for 15 min at room temperature. Then 50 μl of virus particles/magnet were mixed in each well and cells were incubated on a magnet plate for 60 min. The culture plates were removed from the magnetic plate and cells were cultured with or with 1,25-$(OH)_2D_3$ (10^{-8} M) for 7 days. The level of OCL formation was determined by counting the number of $TRAP^+$ multinucleated cells (≥3 nuclei/cell).

Quantitative μCT measurements

The gross morphologic and microarchitectural traits of the distal area of the femur and L_5 vertebra were examined by quantitative μCT. The L_5 vertebrae were used to assess histomorphometry of the trabecular bones, and the femurs were used to measure mean cortical thickness. Specimens were held with Styrofoam within plastic vials and positioned within a 25-mm-diameter acrylic tube. After an initial scout scan, full-length scans were obtained at an isotropic voxel resolution of 10.5 μm using a commercial scanner (Scanco Viva CT40, Scanco Medical AG, Bassersdorf, Switzerland) using the following settings: Energy=55 kVp, current=145 mA, and integration time=300 ms. A total of 300 slices with an increment of 25 μm were obtained on each bone sample starting 1.0 mm below the

growth plate in the area of the secondary spongiosa. The area for analysis was outlined within the trabecular compartment, excluding the cortical and subcortical bone. Every 25 sections were outlined, and the intermediate sections were interpolated with the contouring algorithm to create a volume of interest. Segmentation values used for analysis were sigma 0.8, support 1, and threshold 275. A 3D analysis was done to determine bone volume (BV/TV, %), trabecular number (Tb.N, N/μm^2), trabecular thickness (Tb.Th, μm), and trabecular bone spacing (Tb.Sp, μm). Cortical bone also was analysed in the femur 2 mm below the growth plate, and the same segmentation parameters were used for analysis.

Bone histomorphometric analyses

Prior to sacrifice, mice were given calcein (10mg/kg) on day -7 and day -2 prior to sacrifice. Lumbar vertebrae from 13 TRAP-*TAF12* transgenic mice and 24 wild type mice were subjected to qualitative histological examination and quantitative histomorphometry. The bones were fixed in 10% buffered formalin at 4°C. The 1–4th lumbar vertebrae were decalcified in 10% EDTA at 4°C and embedded in paraffin. The 5th lumbar vertebra was embedded without decalcification in methyl methacrylate. Five-μm frontal sections were cut for both decalcified and undecalcified samples. The decalcified sections were stained for TRAP and OCL containing active TRAP were stained red as described by Liu et al (22). The undecalcified sections were left unstained for the evaluation of fluorescent labels.

All sections were firstly evaluated qualitatively by microscopy to detect any unusual lesions, and then were analyzed by histomorphometry. The analysis was performed on the cancellous bone/marrow compartment between the cranial and caudal growth plates in the vertebral bodies without lesions using the OsteoMeasure XPTM version 1.01 morphometric program (OsteoMetrics, Inc., Atlanta, GA). Osteoclast perimeter (Oc.Pm) was defined as the length of bone surface covered with TRAP-positive, mono- and multi-nuclear cells, cancellous bone volume (BV/TV), trabecular width (Tb.Wi), trabecular number (Tb.N), trabecular separation (Tb.Sp), mineralizing perimeter (Md.Pm), mineral apposition rate (MAR) and bone formation (BFR) were quantified and calculated. All variables were calculated and expressed and calculated according to the recommendations of the ASBMR Nomenclature Committee (23).

Statistical analysis

For all cell culture studies, significance was evaluated using a two-tailed unpaired Student's t-test, with $p<0.05$ considered to be significant.

RESULTS

Effects of antisense to TAF12 on OCL formation in marrow cultures from PD patients that carry the p62^{P392L} mutation and express measles virus nucleocapsid protein (MVNP) in their OCL precursors

We previously reported that expression of TAF12 was higher in OCL precursors from PD patients than from normals (7, 8), and that OCL precursors from PD patients that carried the *p62*^{P392L} mutation linked to PD and also expressed MVNP were hyper-responsive to 1,25-$(OH)_2D_3$ and expressed increased levels of TAF12 (8). Therefore, to determine the contribution of TAF12 to the hyper-sensitivity to 1,25-$(OH)_2D_3$, we transduced a retrovirus construct containing an anti-sense to *TAF12* into MVNP$^+$ OCL precursors from PD patients and normal OCL precursors. The *TAF12* antisense construct decreased TAF12 expression by more than 80% (data not shown) and the 1,25-$(OH)_2D_3$ hyper-sensitivity of the PD OCL precursors (Figure 1), similar to the effects of antisense *MVNP*. The *TAF12* antisense construct had no effect on 1,25-$(OH)_2D_3$ sensitivity in normal marrow cultures.

Overexpression of TAF12 in human CFU-GM is sufficient to enhance 1,25-$(OH)_2D_3$ hyper-sensitivity

We then examined the effects of over-expression of *TAF12* in normal OCL precursors. These experiments allowed a direct assessment of the capacity of increased levels of TAF12 to mediate 1,25-$(OH)_2D_3$ hyper-sensitivity in OCL precursors in vitro and to determine the potential of TAF12 in the development of pagetic OCL.

The cDNA for *TAF12* was synthesized by RT-PCR from OCL precursor cells of PD patients and inserted into a retroviral construct as previously described (7). Either *TAF12*- or *MVNP*-expressing virus was transduced into normal human marrow cells and OCL precursors treated with varying concentrations of 1,25-$(OH)_2D_3$, and the number and characteristics of the OCL formed were determined. Both *MVNP*- and *TAF12*-transduced normal OCL precursors demonstrated about a 2-fold increase of *TAF12* mRNA expression levels (not shown). In addition, both expressed increased levels of *CYP24A1* mRNA compared to EV-transduced OCL precursors when treated with 10^{-11} to 10^{-7} 1,25-$(OH)_2D_3$ (Figure 2A). *TAF12*-transduced cells formed increased numbers of OCL that were hyper-sensitive to 1,25-$(OH)_2D_3$ (Figure 2B and C), but in contrast to MVNP-expressing cells, did not contain increased numbers of nuclei per OCL at low levels of 1,25-$(OH)_2D_3$ (Figure 2B and C) or produce high levels of IL-6 (47±1pg/ml vs. 269±11pg/ml, TAF12- vs. MVNP-transduced cells). The EV-transduced cells did not produce detectable levels of IL-6 (< 5 pg/ml).

We then determined the bone resorbing capacity of *TAF12*-transduced OCL precursors treated with 1,25-$(OH)_2D_3$. OCL formed by *MVNP*-transduced OCL precursors treated with 1,25-$(OH)_2D_3$ had a markedly increased bone-resorbing capacity per OCL, while the bone resorption capacity per OCL formed by *TAF12*-transduced OCL precursors was similar to those from EV-transduced OCL precursors (Figure 2D).

Osteoclast precursors from TRAP-*TAF12* mice display 1,25-$(OH)_2D_3$ hyper-sensitivity

We generated TRAP-*TAF12* transgenic mice in which *TAF12* expression is targeted to the OCL lineage with the TRAP promoter. Four founder mice were obtained, and lines of mice were generated from each. Levels of TAF12 expression in OCL precursors were measured by Western blot and two lines expressing TAF12 comparable to the levels seen in TRAP-*MVNP* mice were selected for further analysis (Figure 3A). Comparable results were obtained from mice of both lines, and all of the results shown here were obtained from mice of line 2. When bone marrow from TRAP-*TAF12* and TRAP-*MVNP* mice was cultured with 1,25-$(OH)_2D_3$ or RANKL, OCL were formed at low concentrations (10^{-10}M) of 1,25-$(OH)_2D_3$ in both lines, a concentration that does not induce OCL formation in marrow from WT mice (Figure 3B), but neither line was hyper-responsive to RANKL. OCL formed from TRAP-*MVNP* marrow exhibited markedly elevated nuclear numbers per OCL in response to 1,25-$(OH)_2D_3$, but the nuclear numbers per OCL in TRAP-*TAF12* mice were similar to WT OCLs (Figure 3C). To determine if these OCL precursors demonstrated enhanced VDR-mediated transcription at low concentrations of 1,25-$(OH)_2D_3$, the expression of *CYP24A1* (a classic 1,25-$(OH)_2D_3$-responsive gene with two VDREs in its promoter) was measured. As shown in Figure 3D, OCL precursors from both TRAP-*MVNP* and TRAP-*TAF12* mice showed increased *CYP24A1* expression compared to WT mice when treated with low concentrations of 1,25-$(OH)_2D_3$. IL-6 production following 1,25-$(OH)_2D_3$ treatment was also increased in OCL precursors from both TRAP-*MVNP* and TRAP-*TAF12* mice compared to wild type mice, but to a lesser extent in the TRAP-*TAF12* OCLs (Figure 3E).

Bone phenotype of TRAP-TAF12 mice

We examined the bone phenotype of TRAP-*TAF12* mice at 12 months of age in the lumbar vertebral bodies by qualitative histology and histomorphometry, and in the femur and 5th vertebra by μ-CT. The histomorphometry studies showed that no pagetic lesions were found in the lumbar vertebral bone of the TRAP-*TAF12* or WT mice. There were no significant differences between the TRAP-*TAF12* and the WT mice in bone structural variables of cancellous bone volume (BV/TV), trabecular number (Tb.N), trabecular width (Tb.Wi) and trabecular separation (Tb.Sp), nor in the osteoclast perimeter, mineralizing perimeter, mineral apposition rate and bone formation rate (Figure 4). The result of μ-CT analysis of the femur and 5th lumbar veretabra revealed no significant differences (Figure 4).

TAF12 binds the *CYP24A1* promoter

ChIP analysis was performed using an anti-TAF12 antibody and primers flanking the two VDREs in the *CYP24A1* promoter in both TRAP-*MVNP* and WT OCL precursors. 1,25-$(OH)_2D_3$ was found to induce TAF12 binding to the *CYP24A1* promoter in TRAP-*MVNP* as well as WT OCL precursors, but with both basal and induced levels of binding much higher in the TRAP-*MVNP* OCL precursors (Figure 5A).

TAF12 interacts with ATF7

Since ATF7 interacts with TAF12, we next determined if ATF7 contributed to the effects of TAF12 on VDR responsivity. Increased levels of ATF7 expression were detected in MVNP compared to WT lysates and were not further increased by 1,25-$(OH)_2D_3$ (Figure 6A). Expression of TAF4 was not affected by MVNP (Figure 6A). Immunoprecipitation of lysates from OCL precursors of either WT or TRAP-*MVNP* with an anti-TAF12 antibody followed by blotting with an anti-ATF7 antibody or vice versa revealed that TAF12 and ATF7 physically interacted in OCL precursors (Figure 6B). We then examined if MVNP increased expression of phosphorylated ATF7 in OCL precursors since phosphorylated ATF7 binds TAF12. Phosphorylated ATF7 levels in MVNP mice were increased 4-fold compared to WT mice at 30 min. (Figure 6C). To clarify the role of ATF7 in the increased VDR responsivity induced by TAF12 and the effects TAF12 binding to VDR/VDRE, ATF7 was knocked-down in OCL precursors from TRAP-*MVNP* and WT with sh*ATF7* RNA. ChIP analysis of ATF7 knock-down in OCL precursors from TRAP-MVNP mice markedly decreased TAF12 binding at the *CYP24A1* promoter than control shRNA transduced osteoclast precursors (Figure 5B). Knockdown of ATF7 in OCL precursors from TRAP-MVNP mice decreased CYP24A1 sensitivity to 1,25-$(OH)_2D_3$ and TAF12 levels in MVNP-expressing cells (Figure 6D). We then examined the role of ATF7 in osteoclast formation stimulated by 1,25-$(OH)_2D_3$. Treatment of OCL precursors from MVNP or WT mice with an *ATF7* shRNA significantly decreased the numbers of TRAP(+) MNC (Figure 6E). Vehicle treated cultures did not form OCL (data not shown).

MVNP and TAF12 enhance VDR content

VDR content in OCL precursors from TRAP-*MVNP* and TRAP-*TAF12* mice treated with 1,25-$(OH)_2D_3$ (10^{-11}M to 10^{-7}M) was markedly increased in both as compared to WT cells (Figure 7A).To determine if MVNP and TAF12 increase the stability of VDR as a mechanism to enhance 1,25-$(OH)_2D_3$ responsivity, we examined VDR half-life in cycloheximide-treated *MVNP*-transfected (*MVNP*-NIH3T3) and *EV*-transfected NIH3T3 cells (*EV*-NIH3T3). VDR content was quantified by Western blot. 1,25-$(OH)_2D_3$ increased VDR content in both cells types, but to the same extent in *MVNP*- and *EV*-transfected cells (Figure 7B). In contrast, transfection of *TAF12* siRNA, decreased VDR content (Figure 7C).

DISCUSSION

We previously reported that OCL precursors from Paget's Disease (PD) patients are hypersensitive to 1,25-$(OH)_2D_3$ and form OCL at physiologic rather than pharmacologic levels of 1,25-$(OH)_2D_3$ (3). We found that the increased 1,25-$(OH)_2D_3$ sensitivity was mediated by TAF12, a novel co-activator of VDR, which plays an important role in the abnormal OCL activity in PD (7). Further, increased expression of *TAF12* in NIH3T3 cells or normal marrow stromal cells also increased their sensitivity to 1,25-$(OH)_2D_3$ (7), indicating that TAF12 can act as a VDR co-activator in multiple cell types. However, the underlying molecular mechanisms and the contribution of TAF12 to OCL activity in both normals and PD patients are unknown.

We examined the effects of blocking *TAF12* expression in OCL precursors from PD patients who harbor the $p62^{P392L}$ mutation and whose OCL also express measles virus nucleocapsid protein (MVNP). We found that treatment with an antisense to *TAF12* resulted in loss of 1,25-$(OH)_2D_3$ hyper-sensitivity in OCL from PD patients, but did not affect normal OCL function *in vitro* (Figure 1). These results demonstrate that TAF12 induced by MVNP enhances the 1,25-$(OH)_2D_3$ responsivity of pagetic OCL precursors and contributes to the pagetic phenotype of OCL from PD patient.

We then determined the effects of overexpression of *TAF12* in normal OCL precursors using retroviral constructs in normal human OCL precursors. This approach allowed a direct assessment of the capacity of increased levels of TAF12 to mediate 1,25-$(OH)_2D_3$ hyper-sensitivity of OCL precursors in vitro and to determine the potential of TAF12 to induce pagetic OCL. Both *MVNP*- and *TAF12*-transduced normal human OCL precursors demonstrated increased expression of *CYP24A1* mRNA and formed increased numbers of OCL in response to 1,25-$(OH)_2D_3$ compared to *EV*-transduced OCL precursors (Figure 2A). However, *TAF12*-transduced OCL did not have increased numbers of nuclei per cell at low levels of 1,25-$(OH)_2D_3$ or produce the high levels of IL-6, which are characteristic of PD. High levels of IL-6 increase nuclear number per OCL and thereby the bone resorbing capacity of the OCLs. This may explain why the bone resorbing capacity of OCL expression TAF12 was not increased compared to *EV*-OCL. These results demonstrate that *TAF12* by itself cannot induce typical pagetic OCL or induce high levels of IL-6, a characteristic of PD. Further, OCL precursors from TRAP-*TAF12* mice, which overexpress TAF12 to a level comparable to that seen in the TRAP-*MVNP* mice, show increased OCL precursors responsivity to 1,25-$(OH)_2D_3$ (Figure 3B and D) and have modestly increased IL-6 production by OCL (Figure 3E), but do not have increased nuclei/OCL (Figure 3C). Further, the TRAP-*TAF12* mice do not develop pagetic OCLs or bone lesions in vivo and structural variables, osteoclast perimeter and dynamic bone formation variables were similar to those in wild type mice (Figure 4). These results demonstrate that TAF12 increases VDR transcriptional activity, but is not sufficient to induce pagetic OCL and bone lesions characteristic of PD.

To dissect the molecular mechanisms responsible for the effects of TAF12 on OCL formation in both WT and TRAP-*MVNP* mice, we performed ChIP analysis using an anti-TAF12 antibody. We demonstrated that TAF12 in the presence of 1,25-$(OH)_2D_3$ binds the *CYP24A1* promoter, which contains two functional VDREs (Figure 5).

Next, we examined the role of ATF7 on TAF12-VDR-mediated OCL activity, and the impact of loss of *ATF7* on OCL precursor responsiveness to 1,25-$(OH)_2D_3$ in vitro. *ATF7* binds as a homodimer to cAMP response element (CRE) sequences (TGACGTCA) and can also heterodimerize with members of the Jun and Fos families to bind TPA response element (TRE) sequences (TGACTCAG) (24–26). Hamard and colleagues (12) reported that

overexpressed *TAF12* directly interacts with *ATF7* and potentiates ATF7-induced transcriptional activation of *ATF7*-driven genes. Thus, TAF12 is a functional partner of ATF7.We detected increased levels of ATF7 expression in MVNP compared to WT OCL precursor lysates that were not further increased by 1,25-$(OH)_2D_3$. Expression of TAF4 was not affected by MVNP (Figure 6A). Co-immunoprecipitation studies revealed that TAF12 and ATF7 physically interact in both TRAP-*MVNP* and WT OCL precursors (Figure 6B), and that the ratio of TAF12 to TAF4 is increased by MVNP, thus enhancing the ATF7-TAF12 interaction. *CYP24A1*, a key VDR target gene, is the first gene activated by VDR and deactivates 1,25-$(OH)_2D_3$ to control the transcriptional activity of VDR (28). We showed that knockdown of ATF7 decreases *CYP24A1* sensitivity to 1,25-$(OH)_2D_3$ as well as TAF12 levels in *MVNP*-expressing cells (Figure 6D), and knockdown of ATF7 in OCL precursors decreased OCL formation stimulated by 1,25-$(OH)_2D_3$ (Figure 6E). However, ATF7 did not bind VDR as shown by GST-VDR pull down assays with OCL lysates (data not shown). Thus, the interaction of ATF7 with TAF12 may be involved in the up-regulation of TAF12 and the resulting hyper-sensitivity of OCL precursors to 1,25-$(OH)_2D_3$. Recently, results presented by Hamard et al. show that ATF7 is sumoylated in vitro and in vivo, which affects its intranuclear localization by delaying its entry into the nucleus (29). Sumoylation of ATF7, which affects its binding capacity to specific sequences within target promoters, was shown to be induced by binding to TAF12 (29). These reports and our results from ChIP assays (Figure 5B) of *AFT7* shRNA-treated osteoclast precursors derived from TRAP-*MVNP* mice show that ATF7 increases TAF12 binding to VDREs and enhances transcriptional activity on *CYP24A1*. We cannot determine from these experiments if the effects of ATF7 or TAF12 binding to CYP24A1 simply reflect changes in the amounts of TAF12 or direct effects of ATF7 on TAF12 binding to *CYP24A1* promoter.

Results obtained using bone marrow from TRAP-*MVNP* and TRAP-*TAF12* mice demonstrated that 1,25-$(OH)_2D_3$ (10^{-12} to 10^{-8} M) markedly increased VDR content when TAF12 expression was increased in TRAP-*MVNP* and *TAF12* mice (Figure 7A). 1,25-$(OH)_2D_3$ also increased also VDR content in both *MVNP*-transfected NIH3T3 cells (*MVNP*-NIH3T3) and empty vector transfected cells (*EV*-NIH3T3) (Figure 7B). Knockdown of *TAF12* decreased VDR content in NIH-3T3 cells expressing *MVNP* (figure 7C). These results suggest that TAF12 also induces VDR transcription to increase VDR content which may contribute to the 1,25-$(OH)_2D_3$ hyper-sensitivity of OCL precursors overexpressing *TAF12*. Although the mechanism by which it does so is unknown. Several possibilities for the roles of TAF12 and ATF7 in VDR mediated transcription are shown in Figure 8. Since ATF7 does not bind VDR directly, it is unclear if TAF12 is recruited to the *CYP24A1* promoter by ATF7 or VDR. It is possible that VDR recruits TAF12, and the TAF12-VDR complex then brings in ATF7 to the VDRE to enhance VDR mediated transcription (Figure 8A). Alternatively ATF7 could bind to an ATF7 site in the *CYP24A1* promoter which cooperates with VDR bound to the VDRE to recruit TAF12 to the promoter to enhance VDR mediated transcription (Figure 8B). Finally, ATF7 may support enhanced VDR-mediated transcription by binding an ATF7 site at a distance from the *CYP24A1* promoter and act either in cis (perhaps at another CYP24A1 regulatory region) or in trans and thereby regulating another gene such as *TAF12* that is directly involved with the VDR-mediated transcriptosome.

Taken together these results demonstrate that ATF7 and TAF12 are required for 1,25-$(OH)_2D_3$ hyper-sensitivity of OCL precursors. Further, increased expression of TAF12 by itself is not sufficient to induce pagetic OCL precursors or pagetic bone lesions in vivo. Thus, TAF12 and other factors induced by MVNP are required for development of PD.

Acknowledgments

This work was supported by NIH Grant R01 AR057310 (GDR), U.S.Army Medical Research and Materials Command DOD W81XWH-12-1-0533 (NK and GDR) and research funds from the Veterans Administration (GDR).

Author's roles: GDR and NK designed the study and wrote the paper; JT, YH, SI, HI, HC and NK performed the experiments; MAS and JJW generated the TRAP-MVNP and TRAP-TAF12 mice, JPB and LM provided PD patient bone marrow samples and expertise on Paget's disease; HZ and DWD performed histological and analysis. JJW, DWD, DLG, GDR and NK participated in data analyses. All authors approved the final version of manuscript.

REFERENCES

1. Kanis, JA. Pathophysiology and treatment of Paget's disease of bone. 2nd edition. London, United Kingdom: Martin Dunitz; 1998. p. 310
2. Maldague B, Malghem J. Dynamic radiologic patterns of Paget's disease of bone. Clin Orthop Relat Res. 1987; 217:126–151. [PubMed: 3103963]
3. Kukita A, Chenu C, McManus LM, Mundy GR, Roodman GD. Atypical multinucleated cells form in long-term marrow cultures from patients with Paget's disease. J Clin Invest. 1990; 85:1280–1286. [PubMed: 2318982]
4. Mengus G, May M, Jacq X, Staub A, Tora L, Chambon P, Davidson I. Cloning and characterization of hTAFII18, hTAFII20 and hTAFII28: three subunits of the human transcription factor TFIID. EMBO J. 1995; 14:1520–1531. [PubMed: 7729427]
5. Mengus G, Gangloff YG, Carré L, Lavigne AC, Davidson I. The human transcription factor IID subunit human TATA-binding protein-associated factor 28 interacts in a ligand-reversible manner with the vitamin D (3) and thyroid hormone receptors. J Biol Chem. 2000; 275:10064–10071. [PubMed: 10744685]
6. Hoffmann A, Roeder RG. Cloning and characterization of human TAF20/15. Multiple interactions suggest a central role in TFIID complex formation. J Biol Chem. 1996; 271:18194–18202. [PubMed: 8663456]
7. Kurihara N, Reddy SV, Araki N, Ishizuka S, Ozono K, Cornish J, Cundy T, Singer FR, Roodman GD. Role of TAF_{II}-17, a VDR binding protein, in the increased osteoclast formation in Paget's Disease. J Bone Miner Res. 2004; 19:1154–1164. [PubMed: 15176999]
8. Kurihara N, Hiruma Y, Yamana K, Michou L, Rousseau C, Morissette J, Galson DL, Teramachi J, Zhou H, Dempster DW, Windle JJ, Brown JP, Roodman GD. Contributions of the measles virus nucleocapsid gene and the SQSTM1/p62(P392L) mutation to Paget's disease. Cell Metab. 2011; 13:23–34. [PubMed: 21195346]
9. Kurihara N, Hiruma Y, Zhou H, Subler MA, Dempster DW, Singer FR, Reddy SV, Gruber HE, Windle JJ, Roodman GD. Mutation of the sequestosome 1 (p62) gene increases osteoclastogenesis but does not induce Paget disease. J Clin Invest. 2007; 117:133–142. [PubMed: 17187080]
10. Kurihara N, Zhou H, Reddy SV, Garcia Palacios V, Subler MA, Dempster DW, Windle JJ, Roodman GD. Expression of measles virus nucleocapsid protein in osteoclasts induces Paget's disease-like bone lesions in mice. J Bone Miner Res. 2006; 21:446–455. [PubMed: 16491293]
11. Hiruma Y, Kurihara N, Subler MA, Zhou H, Boykin CS, Zhang H, Ishizuka S, Dempster DW, Roodman GD, Windle JJ. A SQSTM1/p62 mutation linked to Paget's disease increases the osteoclastogenic potential of the bone microenvironment. Hum Mol Genet. 2008; 17:3708–3719. [PubMed: 18765443]
12. Hamard PJ, Dalbies-Tran R, Hauss C, Davidson I, Kedinger C, Chatton B. A functional interaction between ATF7 and TAF12 that is modulated by TAF4. Oncogene. 2005; 24:3472–3483. [PubMed: 15735663]
13. Voulgari A, Voskou S, Tora L, Davidson I, Sasazuki T, Shirasawa S, Pintzas A. TATA box-binding protein-associated factor 12 is important for RAS-induced transformation properties of colorectal cancer cells. Mol Cancer Res. 2008; 6:1071–1083. [PubMed: 18567809]
14. Kurihara N, Reddy SV, Menaa C, Anderson D, Roodman GD. Osteoclasts expressing the measles virus nucleocapsid gene display a pagetic phenotype. J Clin Invest. 2000; 105:607–614. [PubMed: 10712432]

15. Reddy SV, Scarcez T, Windle JJ, Leach RJ, Hundley JE, Chirgwin JM, Chou JY, Roodman GD. Cloning and characterization of the 5'-flanking region of the mouse tartrate-resistant acid phosphatase gene. J Bone Miner Res. 1993; 8:1263–1270. [PubMed: 8256664]

16. Reddy SV, Hundley JE, Windle JJ, Alcantara O, Linn R, Leach RJ, Boldt DH, Roodman GD. Characterization of the mouse tartrate-resistant acid phosphatase (TRAP) gene promoter. J Bone Miner Res. 1995; 4:601–606. [PubMed: 7610931]

17. Nagy, A.; Gertsenstein, M.; Vintersten, K.; Behringer, R. A Laboratory Manual. 3rd Edition. Cold Spring Harbor, NY, USA: CSHL Press; 2003. Manipulating the Mouse Embryo.

18. Yu S, Franceschi RT, Luo M, Fan J, Jiang D, Cao H, Kwon TG, Lai Y, Zhang J, Patrene K, Hankenson K, Roodman GD, Xiao G. Critical role of activating transcription factor 4 in the anabolic actions of parathyroid hormone in bone. PLoS One. 2009; 4:e7583. [PubMed: 19851510]

19. Yu S, Jiang Y, Galson DL, Luo M, Lai Y, Lu Y, Ouyang HJ, Zhang J, Xiao G. General transcription factor IIA-gamma increases osteoblast-specific osteocalcin gene expression via activating transcription factor 4 and runt-related transcription factor 2. J Biol Chem. 2008; 283:5542–5553. [PubMed: 18171674]

20. Krötz F, de Wit C, Sohn HY, Zahler S, Gloe T, Pohl U, Plank C. Magnetofection--a highly efficient tool for antisense oligonucleotide delivery in vitro and in vivo. Mol Ther. 2003; 7:700–710. [PubMed: 12718913]

21. Hofmann A, Wenzel D, Becher UM, Freitag DF, Klein AM, Eberbeck D, Schulte M, Zimmermann K, Bergemann C, Gleich B, Roell W, Weyh T, Trahms L, Nickenig G, Fleischmann BK, Pfeifer A. Combined targeting of lentiviral vectors and positioning of transduced cells by magnetic nanoparticles. Proc Natl Acad Sci U S A. 2009; 106(1):44–49. [PubMed: 19118196]

22. Liu B, Yu SF, Li TJ. Multinucleated giant cells in various forms of giant cell containing lesions of the jaws express features of osteoclasts. J Oral Pathol Med. 2003; 32:367–375. [PubMed: 12787044]

23. Parfitt AM, Drezner MK, Glorieux FH, Kanis JA, Malluche H, Meunier PJ, Ott SM, Recker RR. Bone histomorphometry: standardization of nomenclature, symbols, and units. Report of the ASBMR Histomorphometry Nomenclature Committee. J Bone Miner Res. 1987; 2:595–610. [PubMed: 3455637]

24. Ivashkiv LB, Liou HC, Kara CJ, Lamph WW, Verma IM, Glimcher LH. mXBP/CRE-BP2 and c-Jun form a complex which binds to the cyclic AMP, but not o the 12-O-tetradecanoylphorbol-13-acetate, response element. Mol Cell Biol. 1990; 10:1609–1621. [PubMed: 2138707]

25. Chatton B, Bocco JL, Goetz J, Gaire M, Lutz Y, Kedinger C. Jun and Fos heterodimerize with ATFa, a member of the ATF/CREB family and modulate its transcriptional activity. Oncogene. 1994; 9:375–385. [PubMed: 8290251]

26. Chatton B, Bahr A, Acker J, Kedinger C. Eukaryotic GST fusion vector for the study of protein-protein associations in vivo: application to interaction of ATFa with Jun and Fos. Biotechniques. 1995; 18:142–145. [PubMed: 7702840]

27. Gazit K, Moshonov S, Elfakess R, Sharon M, Mengus G, Davidson I, Dikstein R. TAF4/4b x TAF12 displays a unique mode of DNA binding and is required for core promoter function of a subset of genes. J Biol Chem. 2009; 284 26286-2696.

28. Li XY, Boudjelal M, Xiao JH, Peng ZH, Asuru A, Kang S, Fisher GJ, Voorhees JJ. 1,25-Dihydroxyvitamin D3 increases nuclear vitamin D3 receptors by blocking ubiquitin/proteasome-mediated degradation in human skin. Mol Endocrinol. 1999; 13:1686–1694. [PubMed: 10517670]

29. Hamard PJ, Boyer-Guittaut M, Camuzeaux B, Dujardin D, Hauss C, Oelgeschläger T, Vigneron M, Kedinger C, Chatton B. Sumoylation delays the ATF7 transcription factor subcellular localization and inhibits its transcriptional activity. Nucleic Acids Res. 2007; 35:1134–1144. [PubMed: 17264123]

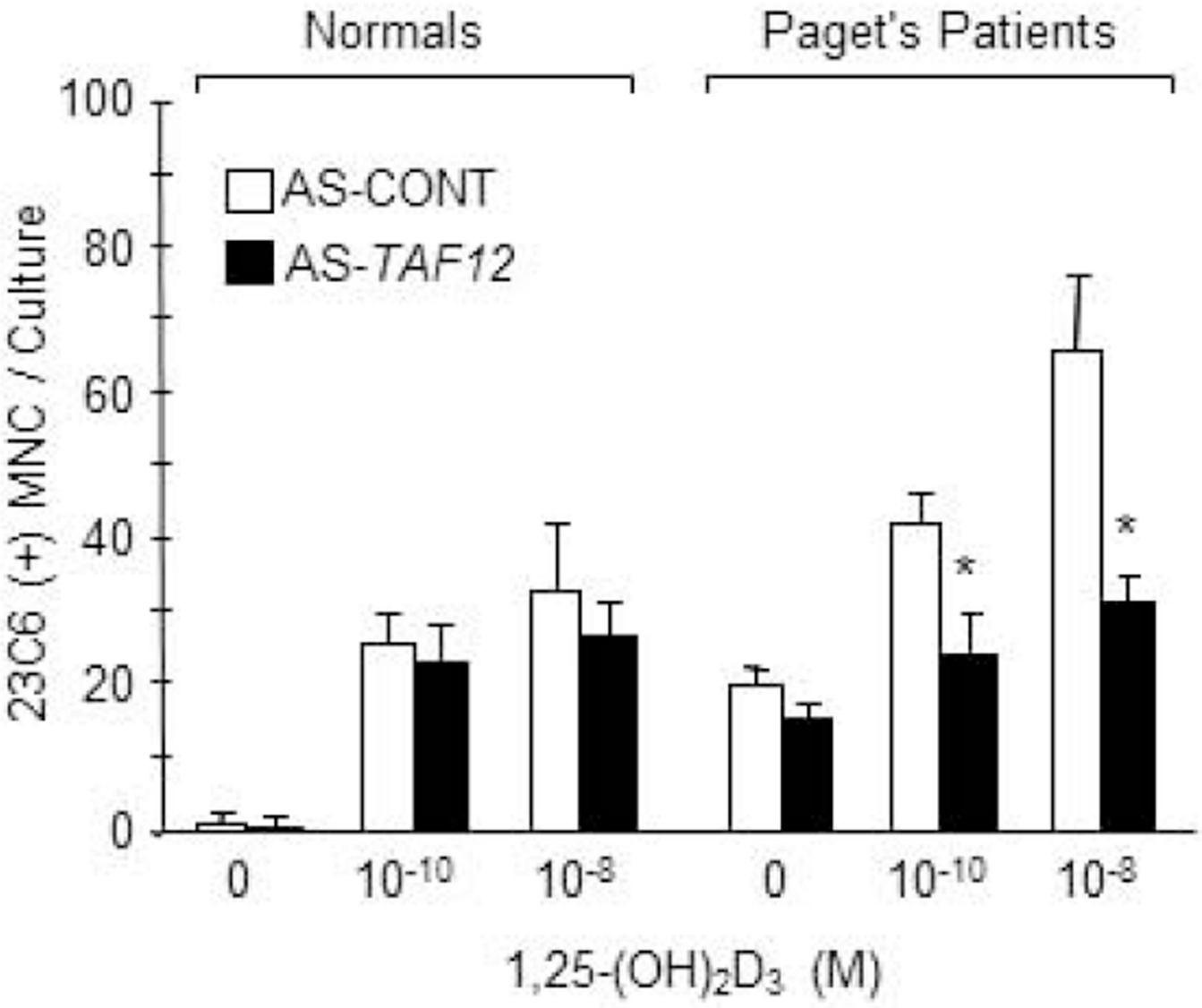

Figure 1. OCL formation stimulated by 1,25-$(OH)_2D_3$ is reduced in antisense TAF12 transduced human OCL precursors from PD patients but not from normals

AS-*TAF12* or scrambled antisense-transduced OCL precursor cells from 3 PD patients or 2 normals were cultured in methylcellulose with recombinant GM-CSF and G418. G418-resistant CFU-GM-derived $CD11b^+$ cells were then cultured with varying concentrations of 1,25-$(OH)_2D_3$ for 3 weeks. The cells were then fixed and stained with the 23C6 monoclonal antibody, which identifies OCL. The results represent the mean ± SD of aggregate data from 3 $MVNP^+$ patients and 2 normals. *, $p<0.01$ compared to scrambled antisense transduced cells.

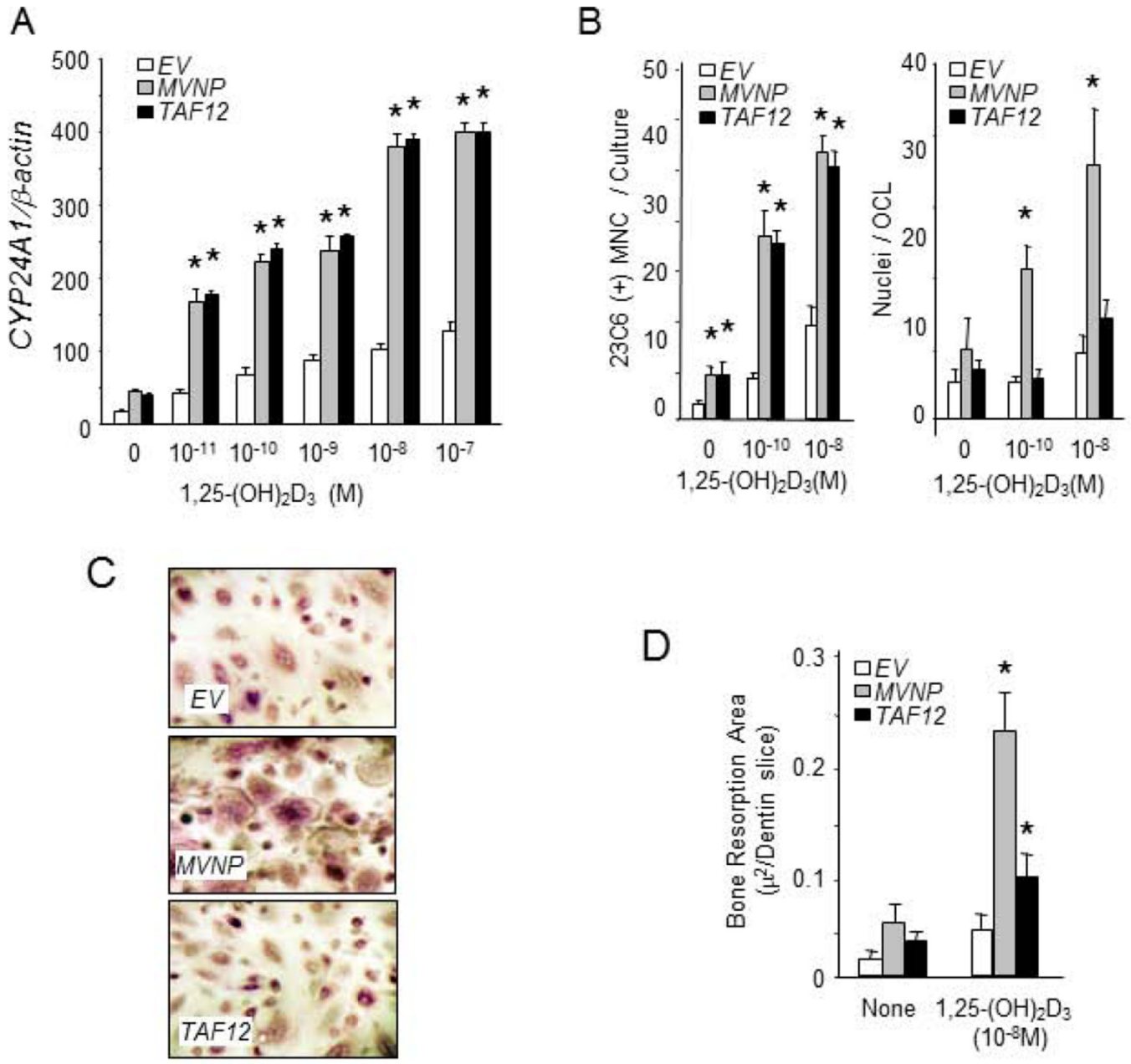

Figure 2. TAF12 enhanced OCL formation, 1,25-$(OH)_2D_3$ sensitivity and bone resorption by normal human OCL precursors transfected with MVNP or TAF12

(A) *CYP24A1 mRNA expressions by human OCL precursors. EV, MVNP* or *TAF12* transduced CFU-GM (5×10^5 cells) were cultured for 2 days with 1,25-$(OH)_2D_3$ and then subjected to RT-PCR analysis for *CYP24A1* mRNA as previously described. The results are expressed as mean ± SD for triplicate cultures. *, $p<0.01$ compared with each concentrations of 1,25-$(OH)_2D_3$ treatment in *EV* transfected cells. **(B)** *Number of 23C6$^+$ multinuclear cells per well. MVNP* or *TAF12* transduced OCL precursors (2×10^5/well) treated with 1,25-$(OH)_2D_3$ formed increased numbers of OCL compared to *EV* transfected cells. The cultures were continued for 3 weeks. The media was replaced two times a week. Multinucleated cells that cross-reacted with the 23C6 antibody and contained 3 or more nuclei were scored as OCLs. Data are expressed as the mean ± SD. (n = 4). *Nuclear number per OCL in marrow*

cultures. The number of nuclei per OCL was determined in 50 random $23C6^+$ OCL for each treatment group in 4 separate cultures, and the results are expressed as mean ± SD. *; Significantly different from the same treatment as cells transfected with *EV*, $p<0.01$. **(C)** 23C6 *staining of formed osteoclasts*. OCL formed from *EV, MVNP* or *TAF12* transduced CFU-GM. OCL precursors were treated with 1,25-$(OH)_2D_3$ for 3 weeks. The media was replaced two times a week. Multinucleated cells that cross-reacted with the 23C6 antibody were scored as OCL (x200). **(D)** *Pit-forming activity of OCLs cultured on dentin slices*. The cultures were overlaid with a dentin slice, and at the end of the culture period, stained with hematoxylin (X200). Bone resorption areas were analyzed by previously described methods (7). Data are expressed as the mean ± SD. (n = 4). *; Significantly different from the same treatment of cells transfected with *EV*, $p<0.01$.

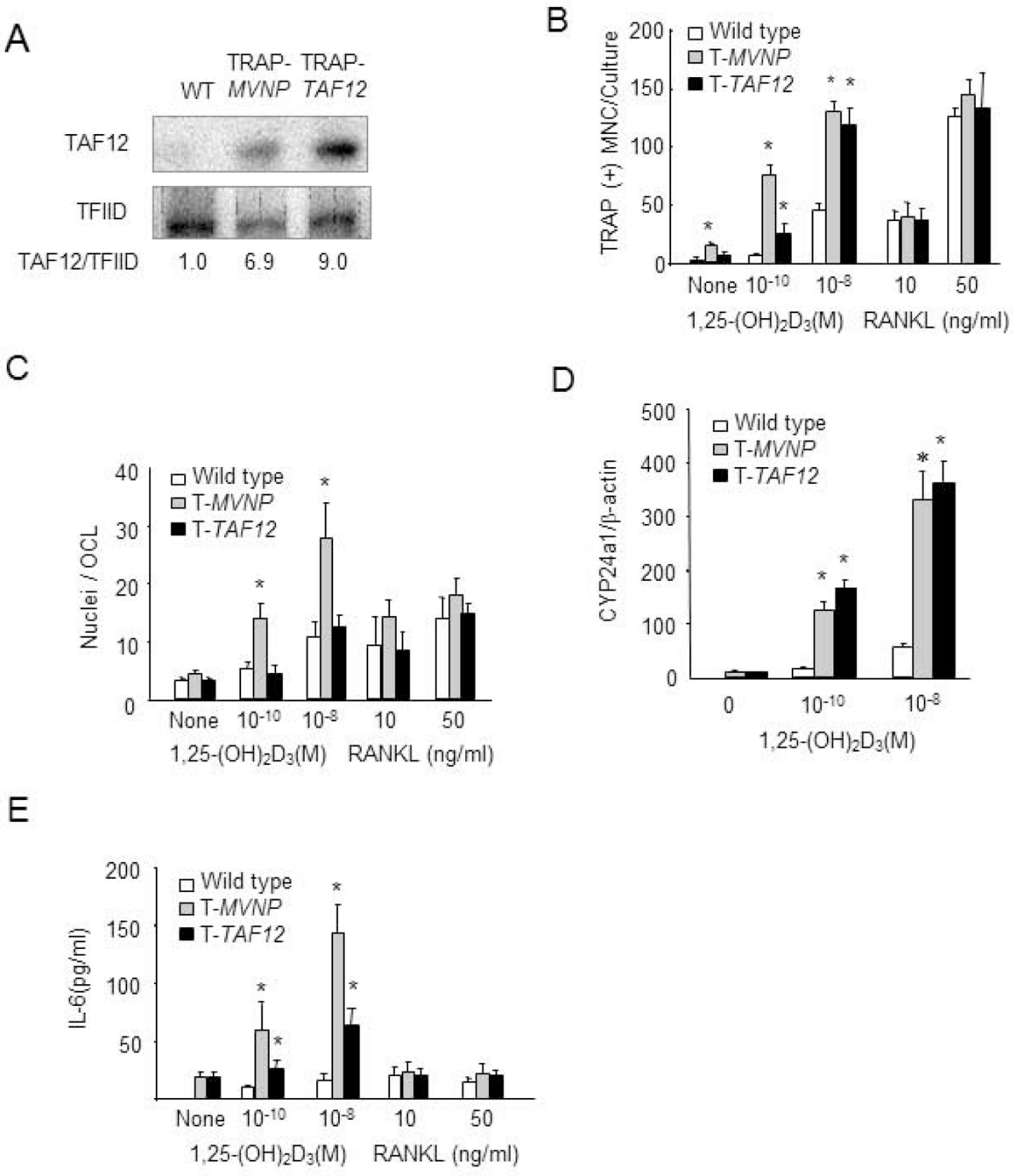

Figure 3. The role of TAF12 in OCL formation by wild-type (WT), TRAP-*MVNP* and TRAP-*TAF12* mice

(A) *TAF12 expression by OCL precursors from TRAP-TAF12 mice*. $CD11b^+$ marrow mononuclear cells from WT, TRAP-*MVNP* and TRAP-*TAF12* mice were cultured for 2 days, then cell lysates were collected. *TAF12* expression was assayed by Western blotting using an anti-TAF12 monoclonal antibody (Protein Tech Group Inc. Chicago, IL). **(B)** *OCL formation by WT, TRAP-MVNP and TRAP-TAF12 mice*. $CD11b^+$ marrow mononuclear cells from WT, TRAP-*MVNP* and TRAP-*TAF12* mice were cultured for 7 days with 1,25-$(OH)_2D_3$ or RANKL and stained for TRAP. Cells with 3 or more nuclei were scored as OCL. Results are expressed as mean ± SD (n=4).*, significantly different from OCL formed

with the same treatment in WT mouse cultures. p<0.01. **(C)** *Nuclear number per OCL in marrow cultures*. The number of nuclei per OCL was determined in 50 random TRAP $^{+}$ OCL for each treatment group in 4 separate cultures, and the results are expressed as mean ± SD. *; Significant different from the same treatment with WT cells, p<0.01. **(D)** *CYP24A1 mRNA expressions by transgenic mouse OCL precursors*. CD11b^{+} marrow mononuclear cells from wild type, TRAP-*MVNP* and TRAP-*TAF12* mice (5×10^5 cells) were cultured for 2 days with 1,25-$(OH)_2D_3$ and then subjected to RT-PCR analysis for *CYP24A1* mRNA. Total RNA from these cells was extracted using RNAzol B solution (TEL-TEST, Inc., Friendswood, TX) and reverse transcribed as follows: 5% of the first-strand cDNA pool was subjected to PCR amplification using real time PCR promoters. The level of *CYP24A1* expression by Taqman QRT-PCR analysis of total RNA isolated from TRAP-*MVNP*, TRAP-*TAF12* or WT cells. PCR was performed for 30 cycles. The gene specific primers for *CYP24A1* mRNA were 5'-CGG GTG GAC CAT TTA CAA CTC GG-3' (sense and 5'-CTC AAC AGG CTC ATT GTC TGT GG-3' (antisense). The gene specific designing primers for *β-actin* were 5'- GTG CGT GAC ATC AAA GAG -3' (sense) and 5'- GCC ACA GGA TTC CAT ACC -3' (Anti-sense). The results are expressed as mean ± S.D. for triplicate cultures. *, $p<0.01$ compared with WT cells. **(E)** *IL-6 production by OCL from transgenic mice*. CD11b^{+} marrow mononuclear cells from wild type, TRAP-*MVNP* and TRAP-*TAF12* mice were cultured for 7 days with 1,25-$(OH)_2D_3$ or RANKL and IL-6 production measured in conditioned media. The production of IL-6 was assayed using specific mouse IL-6 ELISA kit (R &D Company). Results are expressed as mean ± SD (n=4). *, significantly different from OCL formed with the same treatment in WT mouse cultures. p<0.01.

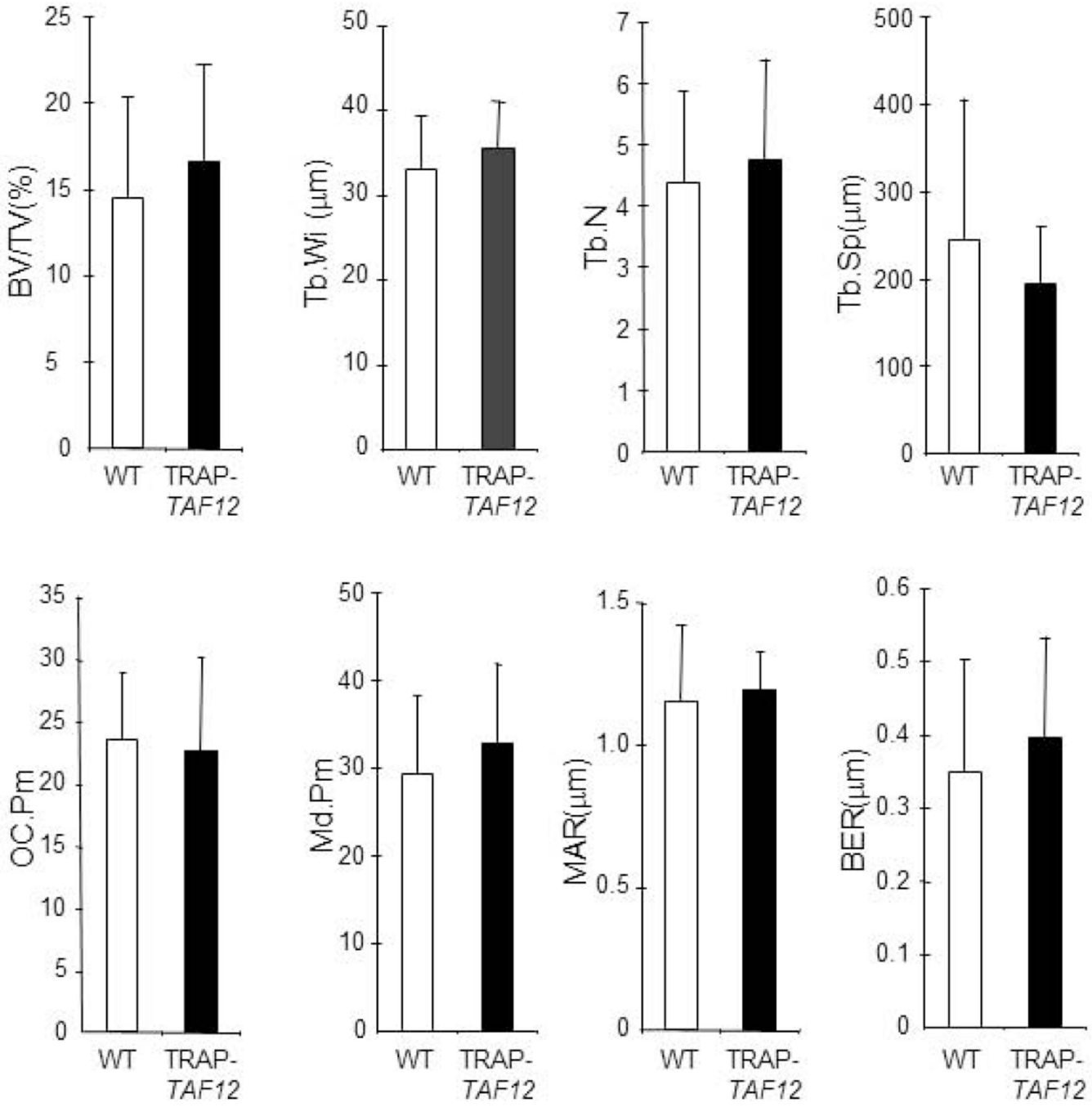

Figure 4. The Quantitation of μCT and histomorphometoric analysis TRAP-*TAF12* and WT mice

The fifth lumbar vertebrae from 12-months of age WT and TRAP-*TAF12* mice was used for these analysis. Bone volume/total bone volume (BV/TV), trabecular number (Tb.N), trabecular thickness (Tb.N), trabecular bone spacing (μm), trabecular bone thickness (2 μm) the OCL surface (OC.Pm), mineralized surface (Md.Pm) mineral apposition (MAR) and bone formation (BFR) rates between TRAP-*TAF12* and WT mice are shown. Data represent mean ± SD for 24 WT and 13 TRAP-*TAF12* mice per group. No significant differences between WT and TRAP-*TAF12* mice were detected.

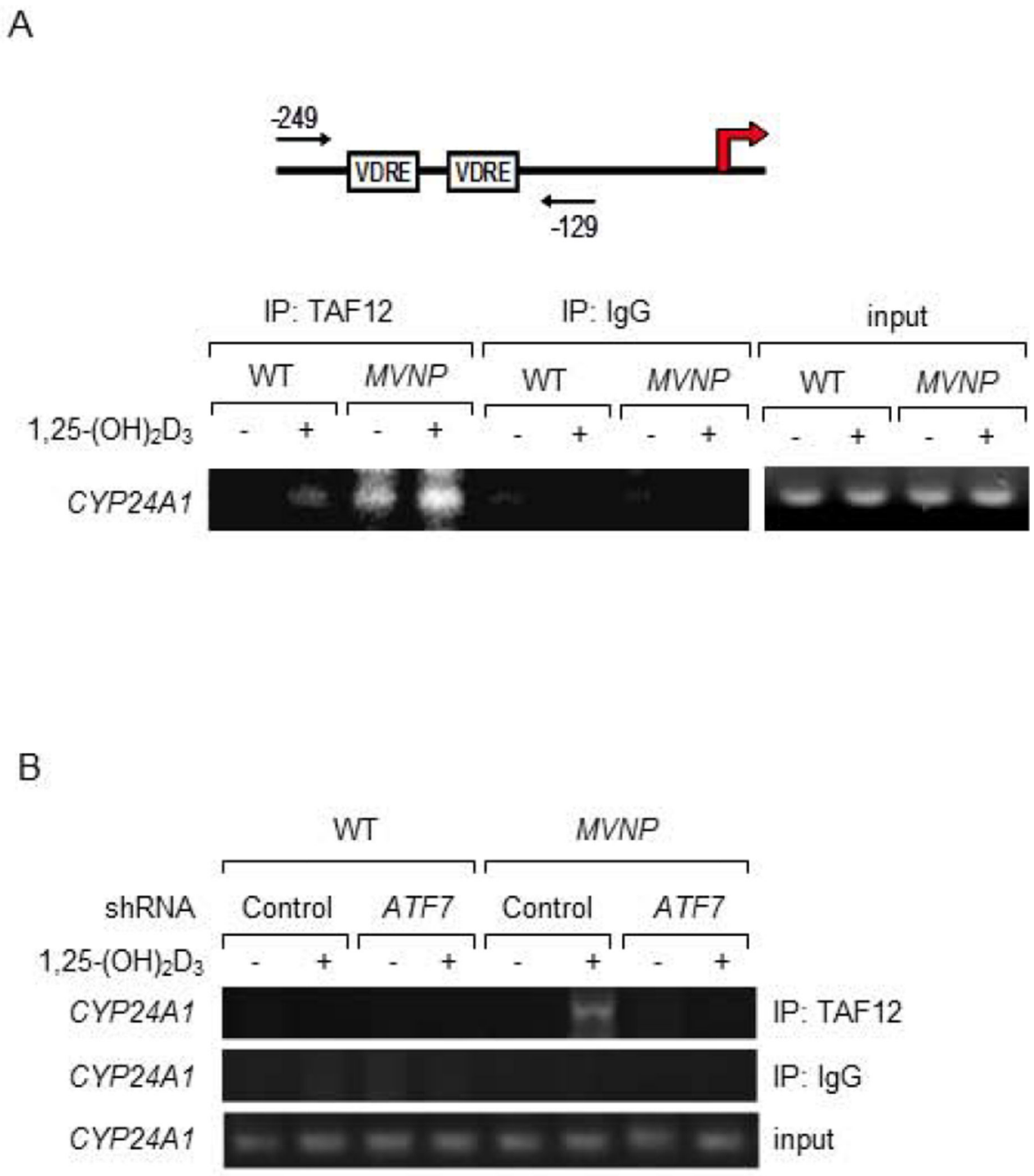

Figure 5. ChIP assay demonstrating that TAF12 binds at the *CYP24A1* promoter in OCL precursors from TRAP-*MVNP* and WT mice

(A) $CD11b^+$ marrow mononuclear cells from wild type and TRAP-*MVNP* mice (1×10^7 cells) were cultured with 1,25-$(OH)_2D_3$ (10^{-8}M) for 24 hours and then subjected to ChIP analysis. ChIP assays were performed using anti-TAF12 (Protein Tech Group) or anti-IgG (Santa Cruz) for control. The mouse *CYP24A1* specific primers were 5'-AAG GAC ACA GAG GAA GAA GCC-3' (sense), 5'- GAA TGG CAC ACT TGG GGT AAG-3' (antisense). **(B)** *Loss of ATF7 decreases TAF12 binding to the CYP24A1 promoter.* CD11b(+) marrow mononuclear cells from wild type and TRAP-*MVNP* mice were transduced with *ATF7*shRNA and cultured with 1,25-$(OH)_2D_3$ (10^{-8}M) for 24 hours and

then subjected to ChIP analysis. ChIP assays were performed using an anti-TAF12 (Protein Tech Group) or anti-IgG (Santa Cruz) for control. The mouse *CYP24A1* specific primers were 5'-AAG GAC ACA GAG GAA GAA GCC-3' (sense), 5'- GAA TGG CAC ACT TGG GGT AAG-3' (antisense).

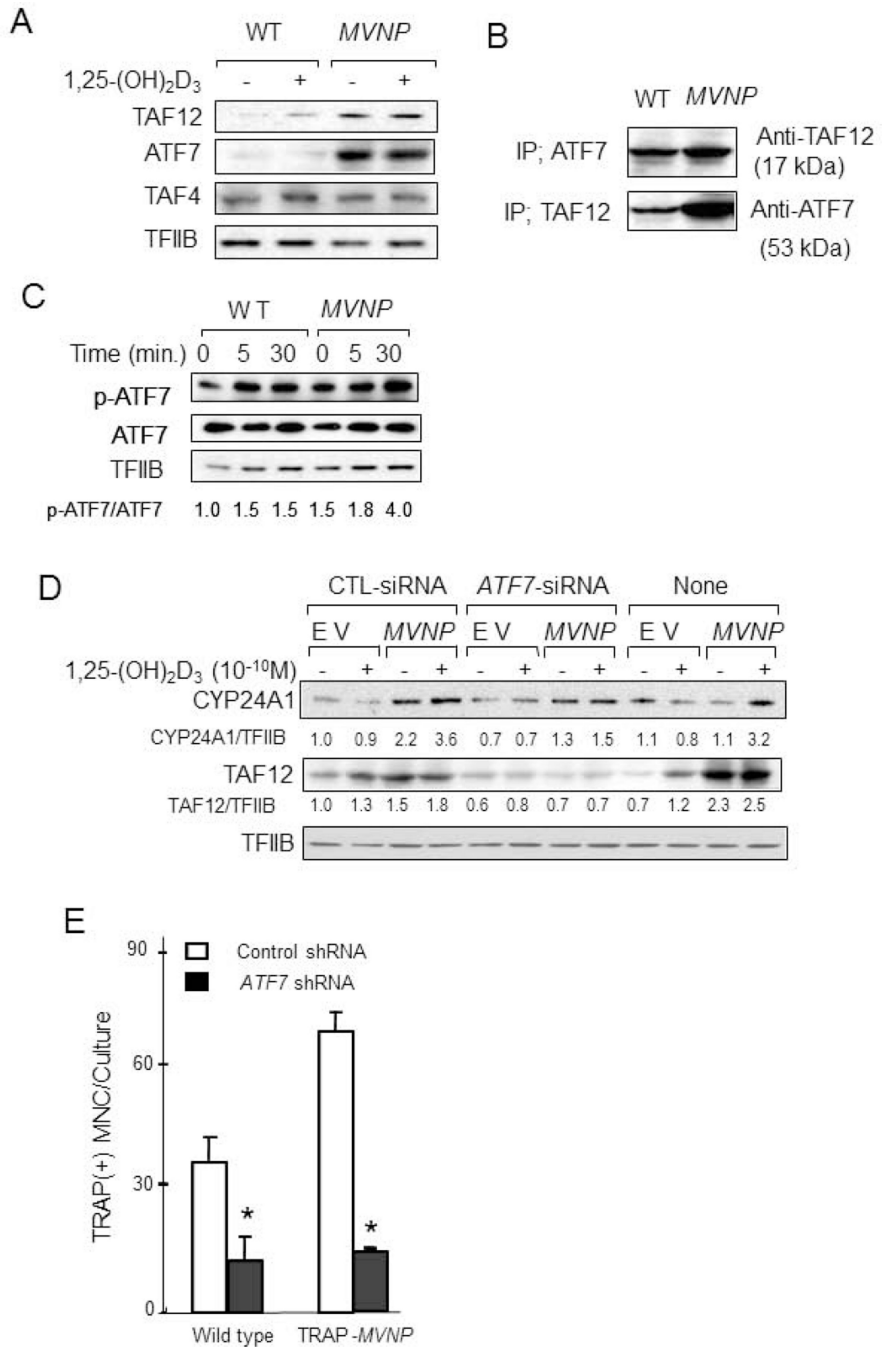

Figure 6. Functional interaction between ATF7 and TAF12

(A) *Expression of TAF12, ATF7 and TAF4 in OCL precursors from WT and TRAP-MVNP mice*. CD11b^{+} marrow mononuclear cells from WT and TRAP-*MVNP* mice were cultured with αMEM-10% FCS for 3 days, and then 10^{-10} M 1,25-$(OH)_2D_3$ or vehicle was added for 48 hours. The cell lysates were collected, the nuclear fraction was isolated using a nuclear isolation kit (Active Motif) and analyzed by Western blot for effects of MVNP on TAF12, ATF7 and TAF4 levels. **(B)** *TAF12 binds ATF7 in OCL precursors*. Cell extracts from WT and TRAP-*MVNP* OCL precursors were immunoprecipitated with an antibody against ATF7 or TAF12, and the immune complexes were analyzed by Western blot with anti-

TAF12 and anti-ATF7, respectively. **(C)** *Analysis of ATF7 activation in MVNP and WT OCL precursors*. $CD11b^+$ marrow mononuclear cells from *MVNP* and WT mice were cultured with 10 ng/ml of M-CSF in 10% FCS and αMEM for 3 days. OCL precursors from transgenic or WT mice were induced with 10^{-8} M of 1,25-$(OH)_2D_3$ for the time periods indicated, the lysates prepared and ATF7 activation determined by Western blot analysis. The nuclear extracts (25 μg of protein/lane) were prepared and subjected to immunoblot analysis using antibodies recognizing anti-phospho ATF7 and anti-ATF7 (Abcam). **(D)** *The role of ATF7 on transcriptional activation of CYP24A1 and TAF12 expression*. ATF7 knockdown experiments were performed with *MVNP* or *empty vector* transduced NIH3T3 cells. Control or *ATF7* siRNA was transduced into NIH3T3 cells and the cells treated with/without 1,25-$(OH)_2D_3$ for 48 hours. CYP24A1 and TAF12 levels were assayed by Western blot using a mouse anti-CYP24A1 or TAF12 monoclonal antibody. The basal ratios of CYP24A1/TFIIB or TAF12/TFIIB are shown as 1.0 for control siRNA transduced *EV*-NIH3T3 without 1,25-$(OH)_2D_3$, and then the value of expression or suppression were calculated and compared to the basal levels. Similar results were seen in three independent experiments. The basal ratio of p-ATF7/ATF7 is shown as 1.0 at 0 min. treatment of WT mice with of 1,25-$(OH)_2D_3$. **(E)** *The role of ATF7 in OCL formation. ATF7* shRNA was transduced into MVNP and WT OCL precursors as described in Material and Methods, the cells cultured for 7 days with 1,25-$(OH)_2D_3$, and then the cells were stained for TRAP. $TRAP^+$ cells with 3 or more nuclei were scored as OCL. Results are expressed as mean ± SD (n=4). *; Significantly different from OCL formed with the same treatment in WT mouse cultures. $p<0.01$.

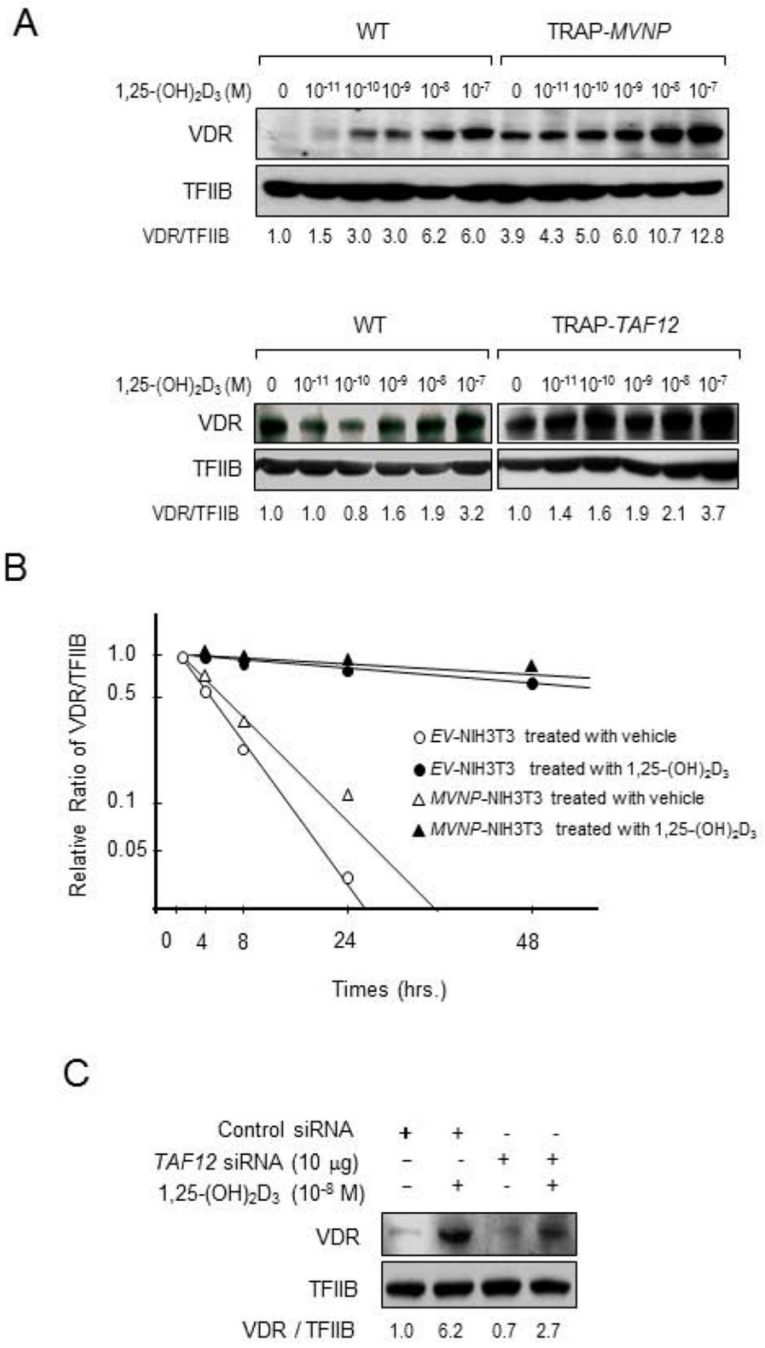

Figure 7. TAF12 increases VDR content

(A) *1,25-(OH)$_2$D$_3$ increased VDR content in OCL precursors from TRAP-MVNP and TRAP-TAF12 mice*. OCL precursor cells from TRAP-*MVNP*, TRAP-*TAF12* mice and WT mice were cultured for 48 hours and amounts of VDR were quantified by Western blot. The basal ratio of VDR/TFIIB is shown as 1.0 for WT cultures without 1,25-(OH)$_2$D$_3$, and then the ratios of VDR expression with 1,25-(OH)$_2$D$_3$ treatment (10^{-11} to 10^{-7} M) were calculated. **(B)** *Effects of 1,25-(OH)$_2$D$_3$ on VDR degradation in EV-NIH3T3 and MVNP-NIH3T3 cells treated with cyclohexamide*. Time-courses for changes in VDR content in the absence or presence of 1,25-(OH)$_2$D$_3$ (10^{-10}M *MVNP*-NIH3T3; 10^{-8}M *EV*-NIH3T3) were

examined in cells treated with cyclohexamide (10 μM). The amount of VDR was quantified by Western blot analysis using a VDR-specific monoclonal antibody. **(C)** *Effects of TAF12 siRNA on VDR content in MVNP-transduced NIH3T3 cells*. Amounts of VDR were quantified by Western blot analysis using a VDR specific antibody after 72 hours. The basal ratio of VDR/TFIIB is shown as 1.0 for control siRNA transduced *MVNP*-NIH3T3 without 1,25-$(OH)_2D_3$, and then the ratios for expression or suppression were calculated.

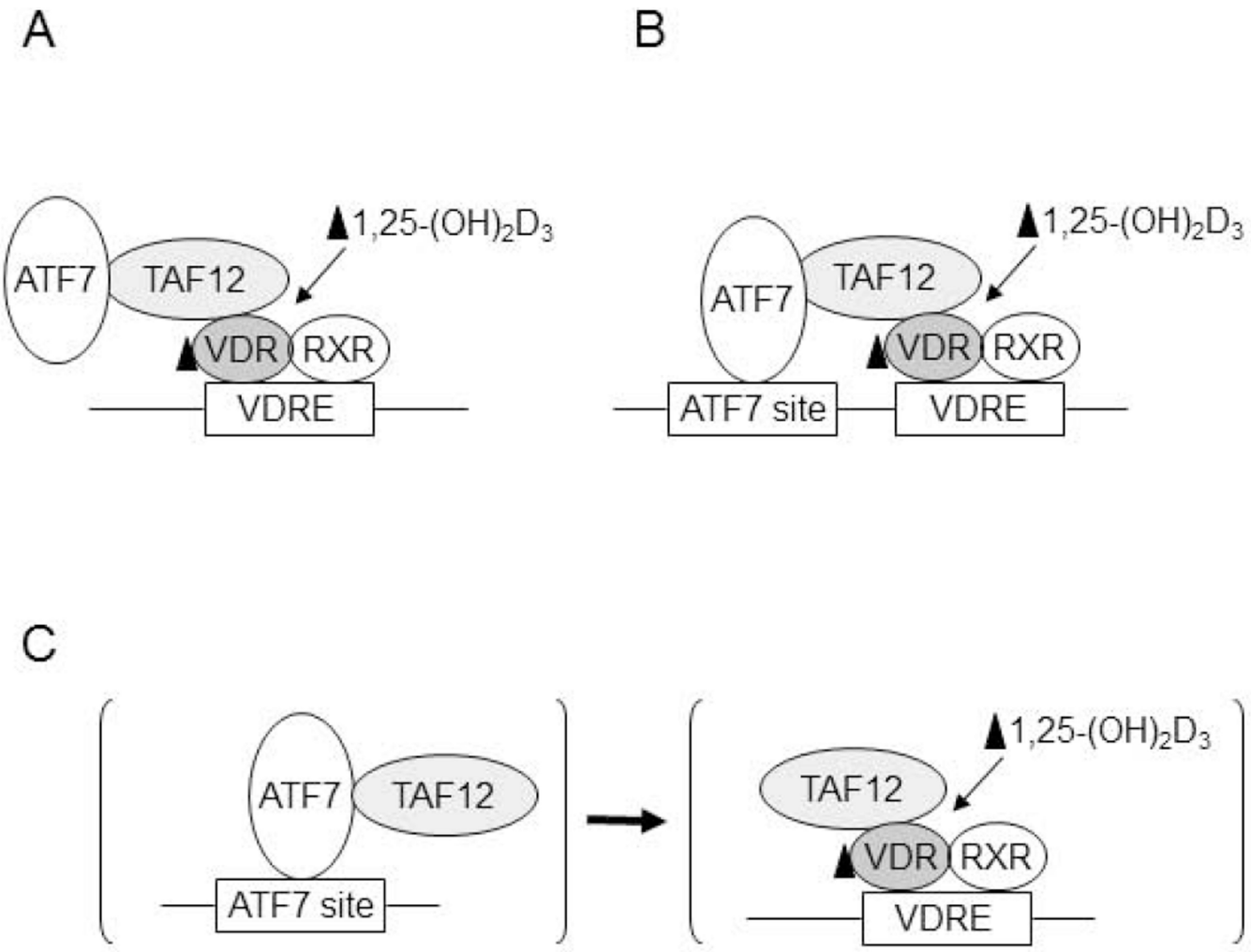

Figure 8. Potential models of TAF12 recruitment to the *CYP24A1* promoter to potentiate VDR activation of transcription

It is unclear if TAF12 recruitment to the *CYP24A1* promoter is via (**A, C**) VDR and/or (**B, C**) ATF7. (**A**) VDR recruits TAF12, which in turn brings in ATF7 and TAF4.(**B**) ATF7 bound to an ATF7 site in the *CYP24A1* promoter and/or VDR bound to the VDRE recruit TAF12•TAF4. (**C**) ATF7 supports enhanced VDR-mediated transcription by acting at a distance from the *CYP24A1* promoter either in cis (perhaps at another CYP24A1 regulatory region) or in trans by regulating another gene such as TAF12 that is directly involved with the VDR-mediated transcriptosome.